



**HAL**  
open science

# Friction Drive Simulation of a Surface Acoustic Wave Motor by Nano Vibration

Minoru Kurosawa, Takashi Shigematsu

► **To cite this version:**

Minoru Kurosawa, Takashi Shigematsu. Friction Drive Simulation of a Surface Acoustic Wave Motor by Nano Vibration. ENS 2007, Dec 2007, Paris, France. pp.8-13. <hal-00202504>

**HAL Id: hal-00202504**

**<https://hal.science/hal-00202504v1>**

Submitted on 7 Jan 2008

**HAL** is a multi-disciplinary open access archive for the deposit and dissemination of scientific research documents, whether they are published or not. The documents may come from teaching and research institutions in France or abroad, or from public or private research centers.

L'archive ouverte pluridisciplinaire **HAL**, est destinée au dépôt et à la diffusion de documents scientifiques de niveau recherche, publiés ou non, émanant des établissements d'enseignement et de recherche français ou étrangers, des laboratoires publics ou privés.



HAL Authorization

**FRICITION DRIVE SIMULATION OF A SURFACE ACOUSTIC WAVE MOTOR  
BY NANO VIBRATION**

*Minoru Kuribayashi Kurosawa<sup>†</sup>, Takashi Shigematsu*

Tokyou Institute of Technology, Yokohama 226-8502, Japan, <sup>†</sup>mkur@ip.titech.ac.jp

**ABSTRACT**

A physical analysis model of a surface acoustic wave (SAW) motor which is driven by frictional force resulted in nano meters elastic vibration has been proposed. In case of the SAW motor, the vibration amplitude is from several nano meters to 30 nm at most. The vibration amplitude is almost same as the elastic deformation caused by preload between a slider and stator. In the analysis model, the elastic deformation, stick and slip were considered. Dynamic simulation was carried out successfully. Experimental results of 9.6 MHz operation frequency SAW motor were compared to the simulation results. It was understood that smaller slider projection slider with a lot of projections has high contact surface stiffness, so that superior performances are obtained in speed and thrust.

**1. INTRODUCTION**

A surface acoustic wave (SAW) motor has been investigated [1]-[4] and demonstrated its superior performances on speed of 1.5 m/s [5], thrust of 10 N [4], and resolution less than 1 nm [6] by using 60x14x1 mm<sup>3</sup> plate piezo transducer. In addition, to enhance application range, higher operation frequency of 100 MHz [7] and two dimensional design [8] were investigated.

From investigations based on experiments, it has been already found that slider surface texture has influence on motor performances such as speed and thrust[3]-[5]. In theoretically, however, the physical property of the slider textured surface on the motor performance has not been investigated enough.

Physical modeling about the SAW motor has been tried, then, one slider projection was modeled including

compliance of slider and stator material [9], and also stick and slip at the boundary. Using the slider projection modeling, operations of SAW motor were simulated, and then, the results were compared with the experimental results.

**2. FRICTION DRIVE MECHANISM**

Surface acoustic wave generated in piezoelectric substrate can be transformed into linear motion through frictional force. If we use Rayleigh wave for the surface acoustic wave actuator, for example, a basic device construction is very simple as shown in Fig. 1. The actuator has only a simple thin plate transducer and a thin friction material.

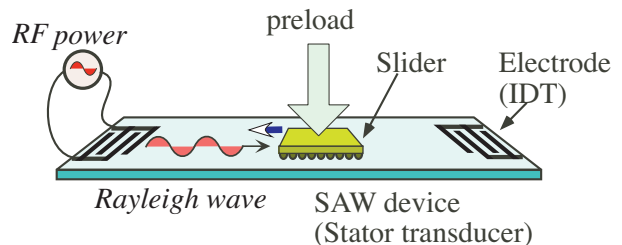


Fig. 1 Schematic of surface acoustic wave motor.

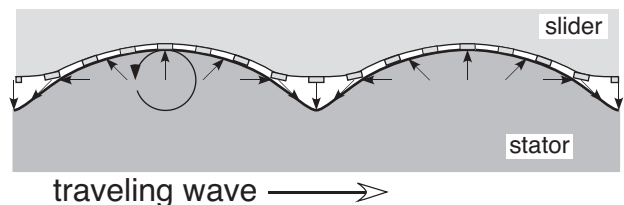


Fig. 2 Schematic drawing of contact between traveling wave in stator and projections on slider surface.

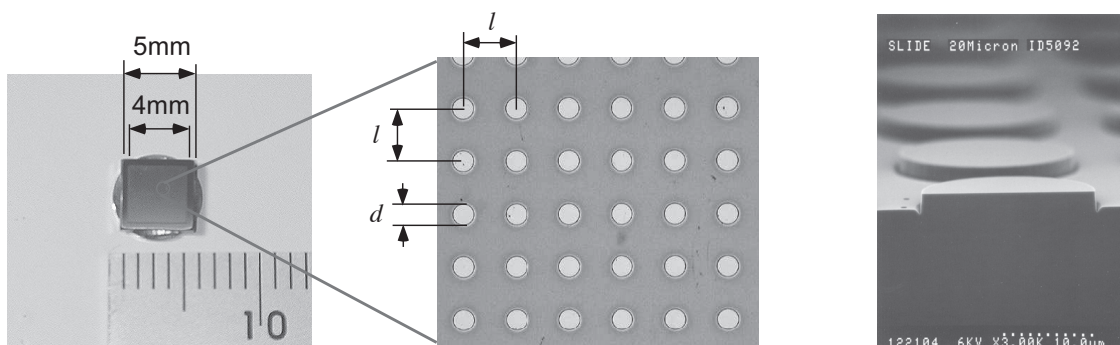


Fig. 3 Photo of silicon slider (left), enhanced view of surface (center) and contact projections on Si slider surface fabricated by dry etching process; SEM view (right).

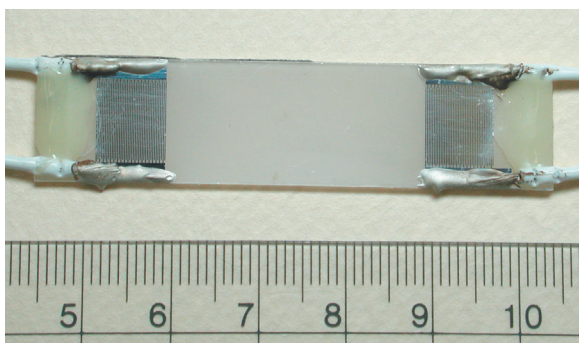


Fig. 4 Photo of SAW transducer for linear motor at 9.6 MHz driven by single electrical source.

The plate transducer is a surface acoustic wave device to generate the Rayleigh wave using two interdigital transducers (IDT) to excite both direction traveling wave. One of the IDTs at a time is driven to excite the wave, and then, to drive the slider in one direction. The active IDT is changed for the alternative linear motion of the slider.

To explain the principle of the actuator driving mechanism, a drawing in which the wave motion is enhanced is convenient to give the image. Actual wave motion is too small to present in the drawing, therefore, the displacement of the wave motion is enlarged about ten thousands times in Fig. 2. In actual dimensions of the wave length and the vibration displacements, the stator surface is almost flat; in case of 9.6 MHz driving frequency, the wave length and the vibration displacements are about 400  $\mu\text{m}$  and 20 nm. In physically, therefore, the contact between the stator and the slider

contains elastic deformation, stick and slip.

The lower part is the SAW transducer and the upper part is the slider. In actual device design, a lot of projections are fabricated, which is mentioned in detail afterward. In the SAW transducer, namely, the stator, the traveling wave is excited. For the friction force which generates the linear motion of the actuator, a pressing force acting on the slider is given, so that the slider is pressing against the stator. This pressing force is called as preload. Due to the wave motion in the stator and the preload on the slider, the boundary between the stator and the slider is distributed as shown in Fig. 2.

The wave motion has two direction components; normal to the boundary and the tangential directions. Due to the wave motion in the stator and the slider stiffness, the pressing force between the slider and the stator has distribution. Hence, around the crest of the wave, the normal force becomes large. On the contrary, at the valley of the wave, the slider surface is off. The large normal force around the wave crest is important for the frictional force in the actuator principle.

At the crest, the particles in the stator have the maximum vibration velocity in the tangential direction which is opposite to the wave traveling direction. The large frictional force and the large tangential vibration velocity generate the linear motion of the actuator. The limit of the actuator speed is the vibration velocity of the wave crest which depends on the vibration amplitude. The limit of the actuator output force is the friction force; at the maxim, the product of the preload and the frictional

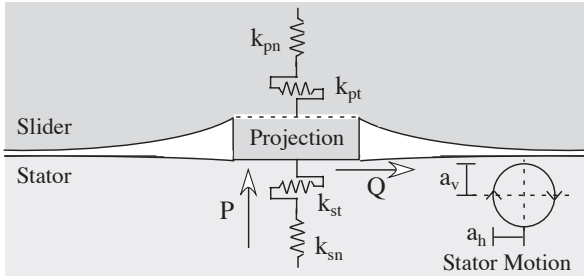


Fig. 5 Physical contact modeling of projection on slider and stator surface.

coefficient between the stator and the slider.

For stable friction drive condition, a lot of projections are fabricated on the surface of the slider as shown in Fig. 3. The diameter of the projections were 20  $\mu\text{m}$  or less to obtain large thrust and high speed close to the vibration velocity in case of 9.6 MHz driving frequency. It has been found from experiments that the larger projection diameters such as 30 or 50  $\mu\text{m}$  resulted lower performance in speed and thrust[4]. For the experiments, several types of silicon sliders were fabricated by dry etching process. The sliders dimensions were 5 by 5  $\text{mm}^2$ ; 2  $\mu\text{m}$  high projections were fabricated in 4 by 4  $\text{mm}^2$  area.

A photo of a SAW motor stator is shown in Fig. 4. The material was 128° y-rotated x-propagation  $\text{LiNbO}_3$ . The dimensions of the device were 60 mm long, 14 mm wide, and 1 mm thick. The electrodes were twenty pair IDTs that were 100  $\mu\text{m}$  wide chromium/aluminum line and 100  $\mu\text{m}$  gap, and 9 mm in aperture. The resonance frequency, namely, the operation frequency was 9.61 MHz. When the driving voltage was 125  $V_{0-p}$ , the vibration amplitude and velocity were 20 nm in normal to the surface and 1.1 m/s in tangential; the input power was 70 W.

### 3. MODELING OF CONTACT

A physical modeling of frictional drive of a SAW motor had been carried out[9] based on contact mechanics[10]. For the first step of the modeling, a slider elastic body, a

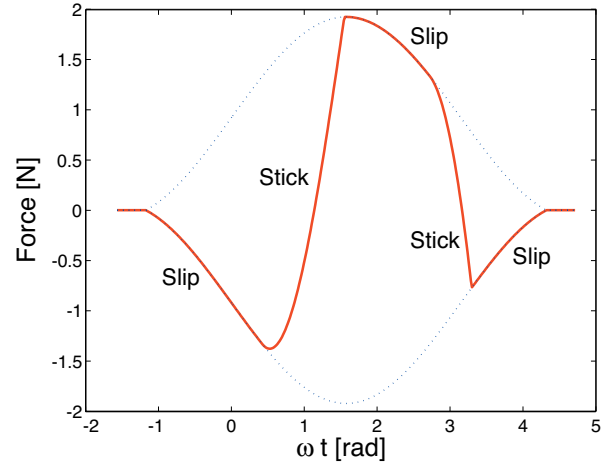


Fig. 6 Force transmission from stator surface to slider with stick and slip.

rigid projection and a stator elastic body were expressed using four springs, one rigid body connected to the elastic slider part and frictional boundary surfaces as shown in Fig. 5.

The two springs in slider  $k_{pn}$  and  $k_{pt}$  can be written in the forms

$$k_{pn} = 4 G_{Si} a (\ln(3-4\nu_{Si}) / (1-2\nu_{Si})) \quad (1)$$

$$k_{pt} = G_{Si} a / (1/8 + (1-2\nu_{Si}) / (8\pi\kappa)) \quad (2)$$

In these equations,  $G_{Si}$ ,  $\nu_{Si}$ , and  $a$  are slider material shear modulus, poisson's ratio and projection radius. In eq (2),  $\kappa = \ln(3-4\nu_{Si}) / \pi$ . The other two springs in stator  $k_{sn}$  and  $k_{st}$  can be written in the forms

$$k_{sn} = 4 G_{LN} a / (1 - \nu_{LN}) \quad (3)$$

$$k_{st} = 8 G_{LN} a / (2 - \nu_{LN}) \quad (4)$$

In these equations,  $G_{LN}$  and  $\nu_{LN}$  are stator material shear modulus and poisson's ratio.

By using the physical model of one projection, a dynamic simulation in time domain was carried out including preload, friction coefficient, vibration amplitude

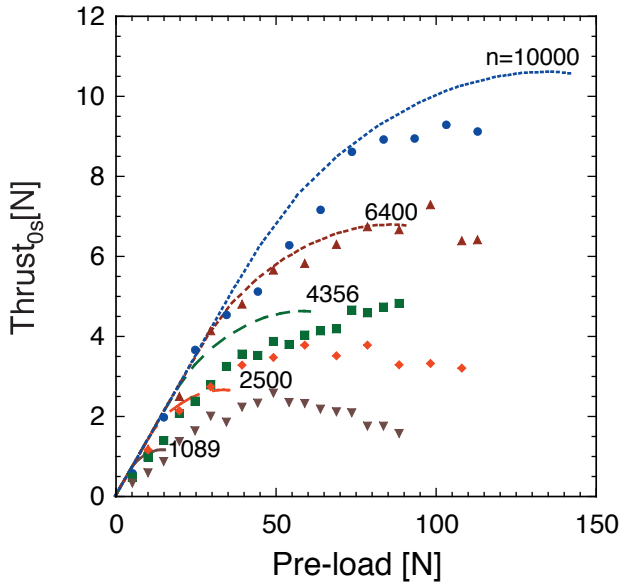


Fig. 7 Output force characteristics of 20  $\mu\text{m}$  diameter sliders by changing the numbers of projections from 100 by 100 to 33 by 33;  $n=10000$  ( $\bullet$ ), 6400 ( $\blacktriangle$ ), 4356 ( $\blacksquare$ ), 2500 ( $\blacklozenge$ ), and 1089 ( $\blacktriangledown$ ).

and so on. From the simulation, dynamic thrust between the stator and slider were obtained as shown in Fig. 6, then, mean speed and thrust of the slider were estimated. It was understood as shown in Fig. 6 that the friction drive has two parts; sticking with elastic deformation in nano-meter range and slipping at the boundaries.

#### 4. ESTIMATION BASED ON PHYSICAL MODEL

Simulations of a SAW motor operation were carried out using the projection contact model and compared to experimental results at 9.6 MHz motor operation mentioned above. The driving voltage was 125  $V_{0-p}$ , so that the vibration amplitude and velocity were 20 nm in normal to the surface and 1.1 m/s in tangential. The slider projection number was change from 1089 to 10000 in case of 20  $\mu\text{m}$  diameter slider. Then, performance difference depending on the slider projection diameter from 20  $\mu\text{m}$  to 50  $\mu\text{m}$  with same contact surface area of about 3  $\text{mm}^2$  in 4x4  $\text{mm}^2$  were compared.

The motor performance improved by increase of the slider projection amount as shown in Figs 7 and

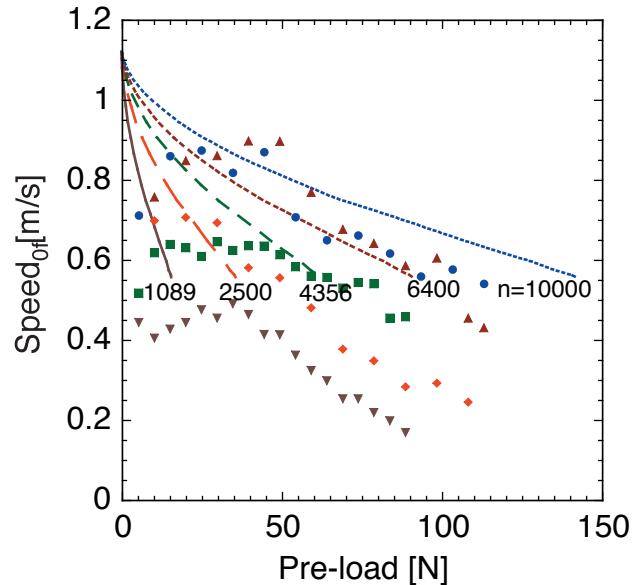


Fig. 8 No-load speed characteristics of 20  $\mu\text{m}$  diameter sliders by changing the numbers of projections from 100 by 100 to 33 by 33;  $n=10000$  ( $\bullet$ ), 6400 ( $\blacktriangle$ ), 4356 ( $\blacksquare$ ), 2500 ( $\blacklozenge$ ), and 1089 ( $\blacktriangledown$ ).

8. We prepared five different slides that had projection amount of 10000, 6400, 4356, 2500 and 1089; projection diameter was 20  $\mu\text{m}$ . In case of 10000 projections, contact surface area was about 3  $\text{mm}^2$  in 4x4  $\text{mm}^2$ . However in the simulation, effective amount of the projections was reduced to 36 % of the actual amount of the projections. This is because the FEM analysis of the static contact of the slider indicated that the projection contact had significant distribution.

The thrust at 0 speed, namely maximum thrust, depends on the pre-load and the amount of the projections as indicated in Fig. 7. From the simulation, it is understood that the stiffness at slider contact surface is important for large thrust. This is because the stiffness is in proportion to the amount of projections. The stiff surface is suitable for high speed operation as can be seen from Fig. 8. In case of soft slider surface, the projections contact to the bottom of the wave by large pre-load.

The difference of the slider projection diameter on the output force of the SAW motor indicated interesting result as shown in Fig. 9. The small diameter projections

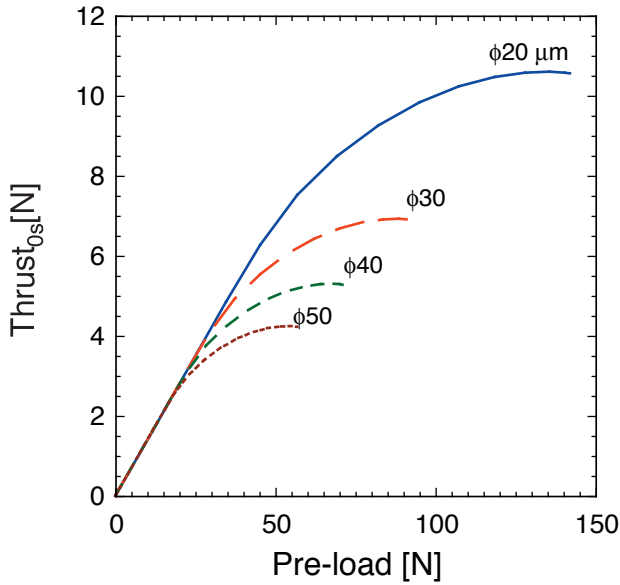


Fig. 9 Output force characteristics difference between 20, 30, 40, and 50  $\mu\text{m}$  diameter sliders by simulation.

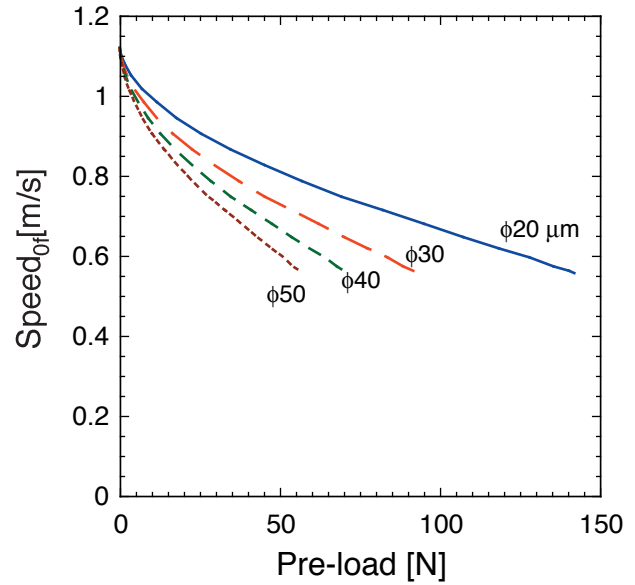


Fig. 10 No-load speed characteristics difference between 20, 30, 40, and 50  $\mu\text{m}$  diameter sliders by simulation.

has lower stiffness than that of large projections. However, the total stiffness becomes higher if the total projection area is same. It is clearly indicated in eqs from (1) to (4) that the stiffness is in proportion to the radius of projections, not to the square of projection radius. So that, if the total projection areas are same, the smaller projection slider has higher surface stiffness. The high surface stiffness of slider conduces large thrust. The higher surface stiffness by small diameter projections brings superior performance in speed also as shown in Fig. 10.

It is clearly understood also from the experintal results that the 20  $\mu\text{m}$  diameter slider has superior performances than that of 50  $\mu\text{m}$  diameter slider in speed and thrust against the variation of the preload as shown in Figs. 11 and 12. Two slider had same contact area of 3  $\text{mm}^2$  but different diameter, so that the different contact stiffness. Each projection contact stiffness is 2.5 times larger, in case of 50  $\mu\text{m}$  diameter slider, but the amount of the projection is  $1/2.5^2$  that of 20  $\mu\text{m}$  diameter slider. As a result, the 50  $\mu\text{m}$  diameter projection slider has 2.5 times lower stiffness. As a result, the smaller diameter projection slider has high contact stiffness.

## 5. CONCLUSION

It had been unclear that the reason why the smaller diameter projection slider has superior performances in speed and thrust for several years. From the physical modeling of SAW motor based on the contact mechanics, the motor operation has successfully explained about the difference of the slider surface texture.

The stiffness of the slider surface depends on the projection diameter and the amount of projections; the smaller diameter slider has stiff surface if the contact areas are same. This is because the stiffness of one projection is in proportion to the projection radius, not the square of the radius. The smaller projection slider, therefore, has high surface contact stiffness in total, so that the smaller projection slider has superior performances in speed and thrust.

It is not examined about the difference of the wave form as indicated in Fig. 6 in this paper. From the physical analysis model of the SAW motor, the dynamics between slider and stator will be examined in time domain. For the efficiency and wear, stick and slip of dynamic

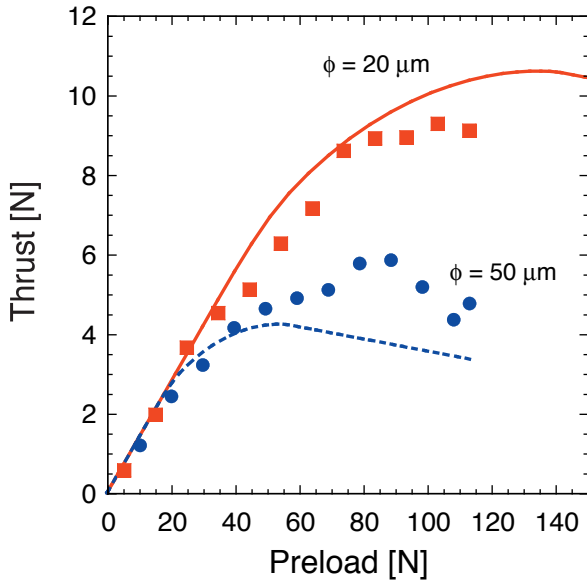


Fig. 11 Output force characteristics difference between 20  $\mu\text{m}$  diameter slider (■) and 50  $\mu\text{m}$  diameter slider (●).

operation condition are important factor. The total design methodology of slider surface will be important research subject. The key will be the elastic deformation of the materials in nano meter range at boundary surfaces.

#### ACKNOWLEDGMENT

This work was supported by a Grant-in-Aid for Science Research from the Ministry of Education, Culture, Sports, Science and Technology, and by a Collaborative Development of Innovative Seeds, Potentiality verification stage from the Japan Science and Technology Agency.

#### REFERENCES

[1] M. Kurosawa, M. Takahashi, and T. Higuchi, "Ultrasonic linear motor using surface acoustic wave," *IEEE Trans. on UFFC*, vol. 43(5), pp. 901-906, 1996.

[2] M. K. Kurosawa, M. Takahashi and T. Higuchi, "Elastic Contact Conditions to Optimize Friction Drive of Surface Acoustic Wave Motor," *IEEE Trans. on UFFC*, vol. 45, no. 5, pp. 1229-1237, 1998.

[3] K. Asai, M. K. Kurosawa and T. Higuchi, "Evaluation of the driving performance of a surface acoustic wave linear

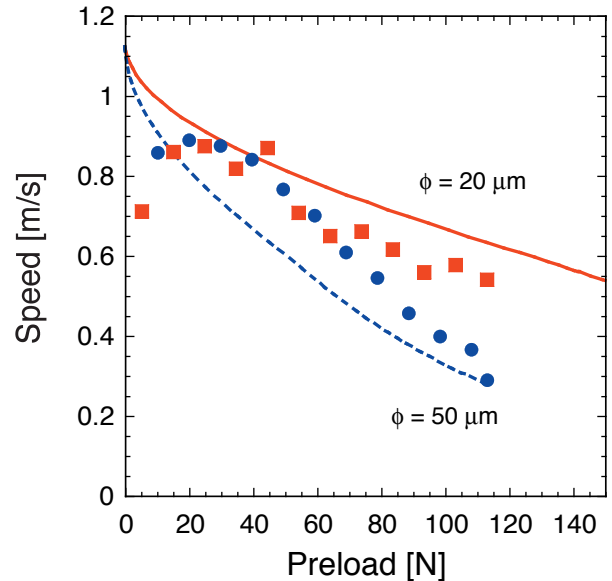


Fig. 12 No-load speed characteristics difference between 20  $\mu\text{m}$  diameter slider (■) and 50  $\mu\text{m}$  diameter slider (●).

motor," *Proceedings of the IEEE Ultrasonics Symp.*, pp. 675-679, 2000.

[4] M. K. Kurosawa, H. Itoh, K. Asai, M. Takasaki, and T. Higuchi, "Optimization of slider contact face geometry for surface acoustic wave motor," *Proc. of IEEE MEMS Conference*, pp. 252-255, 2001.

[5] Y. Nakamura, M. K. Kurosawa, T. Shigematsu and K. Asai, "Effects of ceramic thin film coating on friction surfaces for surface acoustic wave linear motor," *Proc. of the IEEE Ultrasonics Symposium*, pp. 1766-1769, 2003.

[6] T. Shigematsu, M. K. Kurosawa and K. Asai, "Nanometer stepping drive of surface acoustic wave motor," *IEEE Trans. on UFFC*, vol. 50, no. 4, pp. 376-385, 2003.

[7] T. Shigematsu and M. K. Kurosawa, "Miniaturized SAW Motor with 100MHz Drive Frequency," *IEEJ Trans. on Sensors and Micromachines*, vol. 126, no. 4, pp.166-167, 2006.

[8] T. Iseki, T. Shigematsu, M. Okumura, T. Sugawara and M. K. Kurosawa, "Two-dimensionally self-holding deflection mirror using surface acoustic wave motor," *Optical Review*, vol. 13, no. 4, pp. 195-200, 2006.

[9] T. Shigematsu and M. K. Kurosawa, "Friction drive modeling of SAW motor using classical theory of contact mechanics," *Proc. of 10th Conf. on New Actuators*, pp. 444-448 (2006)

[10] K. L. Johnson, *Contact Mechanics*, Cambridge University Press, Cambridge, 1985.